

Article

Spatiotemporal Evaluation of Blue and Green Water in Xinjiang River Basin Based on SWAT Model

Xudong Zhang¹, Cong Jiang^{1,2,*} , Junzhe Huang¹, Zhenyu Ni¹, Jizhou Sun¹, Zuzhong Li¹ and Tianfu Wen²¹ School of Environmental Studies, China University of Geosciences, Wuhan 430078, China² Jiangxi Provincial Institute of Water Sciences, Nanchang 310029, China

* Correspondence: jiangcong@cug.edu.cn

Abstract: Poyang Lake is the largest freshwater lake in China. As an important tributary of Poyang Lake, Xinjiang River has an important influence on the water ecology and water resources of the Poyang Lake basin. Based on the hydrological simulation of the SWAT (Soil and Water Assessment Tool) model, the spatiotemporal distribution and evaluation of the blue and green water during the period (1982–2016) in the basin were explored by the Mann–Kendall test, precipitation anomaly percentage, and scenario simulation. It is found that the SWAT model presents a satisfactory performance in runoff simulation of the basin. The multi-year average blue water in the Xinjiang River basin is 1138 mm, and the green water is 829 mm, with a green water coefficient of 0.42. The amount of blue water in wet years is about 1.5 times that in normal years and 2.4 times that in dry years. Compared with the green water, the blue water of the basin is more sensitive to the variations in precipitation. In spatial distribution, the blue and green water in the middle of the basin is obviously more than those in other parts of the basin. During the study period, the blue water in the basin shows a slight decreasing trend, and the green water shows a significant decreasing trend. It is also found that climatic factors have a greater influence on the trend of blue and green water than land use, and the decrease in precipitation is the dominant cause for the trend of blue and green water.



Citation: Zhang, X.; Jiang, C.; Huang, J.; Ni, Z.; Sun, J.; Li, Z.; Wen, T. Spatiotemporal Evaluation of Blue and Green Water in Xinjiang River Basin Based on SWAT Model. *Water* **2022**, *14*, 2429. <https://doi.org/10.3390/w14152429>

Academic Editor: Liudmila S. Shirokova

Received: 6 July 2022

Accepted: 3 August 2022

Published: 5 August 2022

Publisher's Note: MDPI stays neutral with regard to jurisdictional claims in published maps and institutional affiliations.



Copyright: © 2022 by the authors. Licensee MDPI, Basel, Switzerland. This article is an open access article distributed under the terms and conditions of the Creative Commons Attribution (CC BY) license (<https://creativecommons.org/licenses/by/4.0/>).

Keywords: SWAT; blue water; green water; spatiotemporal distribution; trend analysis; Xinjiang River Basin

1. Introduction

Water is an indispensable resource to sustain human life and development. With the increasing population and rapid socio-economic development, human consumption of freshwater resources is increasing, and the imbalance between supply and demand of water resources not only restricts the balance of the ecosystem but also affects the sustainable socio-economic development and, therefore, is drawing increasing attention [1,2]. The current studies pay more attention to the surface streamflow, which can be directly used, but ignore the evaluation of ecological water [3,4]. In order to evaluate the role of water resources in the ecosystem more comprehensively, Falkenmark put forward the concept of blue water and green water and brought them into the consideration of water resources management [5]. The concept of blue and green water broadens the vision of water resources evaluation and research, especially the proposal of green water, which closely links the whole hydrological cycle system with the ecological cycle system [6,7]. In 2006, the concept of blue and green water was further improved by Falkenmark [8], which classified surface runoff, subsurface runoff, and interflow as blue water, classified the evapotranspiration of the land surface, vegetation, water area, and soil as green water flow, and classified the water content of the soil as green water storage. The sum of green water flow and green water storage is the so-called total green water. As the main part of water consumption, green water is a more active part of the land and water cycle system than blue water, and it plays an extremely important role in maintaining the balance, health, and stability of the global ecosystem [9,10].

As water consumption increases, it is projected that 1.8 billion people could face water shortages by 2025 [11,12]. Quantitative assessment of the availability and vulnerability of blue and green water plays a critical role in sustainable water resources management [13]. For example, Veettil et al. established the SWAT model in the Savannah River Basin of the United States and then quantitatively evaluated the water security of the basin based on the concept of blue and green water [12]. Rodrigues et al. proposed a watershed water security assessment method by quantifying the availability of blue and green water [14].

In the past few decades, human activities have had a strong impact on climate conditions, resulting in significant changes in precipitation, temperature, and other climate conditions, which would further affect the regional hydrological cycle and aggravate the shortage of blue and green water [15,16]. Meanwhile, the high intensity of human activities has changed the land use and land cover, resulting in significant changes in hydrological processes, such as infiltration and evaporation, which would also induce the imbalance between the supply and demand of the blue and green water [17,18]. A quantitative analysis of the impact of climate conditions and land use on blue and green water is of great significance for formulating scientific and reasonable water resources management methods [19,20]. Zuo et al. quantitatively evaluated the availability of blue and green water in different spatial scales of the Weihe River basin in China [21]. Lyu et al. conducted a detailed study on the spatial and temporal distribution characteristics of blue and green water in the Dongjiang River basin based on the SWAT model [3]. These studies on blue and green water can provide a valuable theoretical basis for regional water resources planning and management [22–25].

Poyang Lake, which is located on the southern bank of the middle and lower reaches of Yangtze River, is the biggest freshwater lake in China. It plays an irreplaceable role in regulating floods of Yangtze River, ensuring water supply for its surrounding areas, and providing a habitat for many endangered species [26]. There are many research studies on Poyang Lake, but they mainly focus on water quantity changes and the ecological environment [27–29]. Xinjiang River is an important tributary of Poyang Lake, and a change in its water resources can have a great influence not only on Poyang Lake but also on the regional ecological environment and economic development. However, the current research on water resources in the Xinjiang River basin is mainly focused on surface runoff and sediment [30], while the blue and green water in the basin is seldom addressed. Given what was mentioned above, we established the SWAT model in the Xinjiang River basin. Based on the simulation results of the model, we conducted a quantitative evaluation of the volumes and spatial distribution characteristics of the blue and green water on average in multiple years and in the typical years, and we also carried out an analysis of the variation trend of the blue and green water. Meanwhile, we set up a scenario simulation and studied the impacts of meteorological changes and land use changes on the blue and green water. It is hoped that the research results can provide a scientific basis for the watershed management and water resources planning in the Poyang Lake basin and Xinjiang River basin.

2. Study Area and Data

2.1. Study Area

Xinjiang River is located in the northeast of the Poyang Lake basin. The longitude and latitude are between $116^{\circ}38' E$ – $118^{\circ}36' E$ and $27^{\circ}33' N$ – $28^{\circ}59' N$, respectively (Figure 1). It has a total length of 313 km and a catchment area of about 17,600 km². Meigang hydrological station controls a catchment area of 15,319 km², accounting for about 87% of the total area of the Xinjiang River basin. The upstream part of the Xinjiang River basin is dominated by hills, the midstream part of the basin is a basin, downstream of the basin are alluvial plains, and the elevation of the whole basin is about 16–2136 m. The basin is located in the subtropical monsoon humid climate zone, with a mild climate and abundant rainfall. The annual average temperature is 17.6 °C, and the annual average precipitation is 1876 mm.

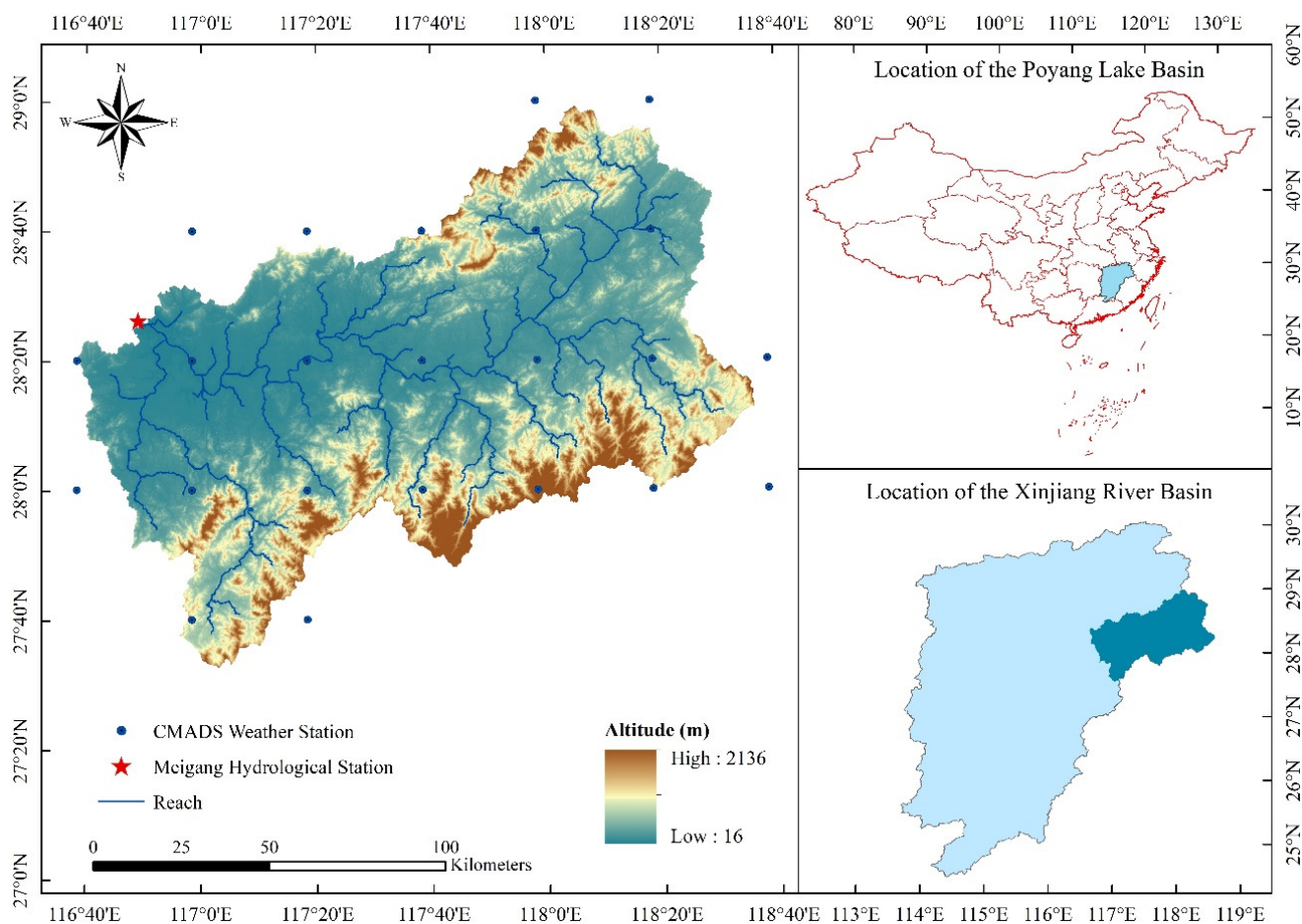


Figure 1. Distribution of Xinjiang River basin location, meteorological stations, and hydrological stations.

2.2. Data

The construction of the SWAT model requires topographic data, land use data, soil data, meteorological data, and hydrological data. The topographic data used in this study are from the Geospatial Data Cloud, with a resolution of 90 m (<https://www.gscloud.cn/>, accessed on 23 March 2022). Land use data of 1990 and 2010 were downloaded from the Resource and Environmental Science and Data Center platform of the Chinese Academy of Sciences (<https://www.resdc.cn/>, accessed on 24 March 2022). Soil data were obtained from the Harmonized World Soil Database v1.2 (HWSD) (<https://www.fao.org/>, accessed on 19 March 2022). The observed daily runoff data of the Meigang hydrological station from 1979 to 2016 were obtained from the Jiangxi Provincial Bureau of Hydrology.

The meteorological data used are CMADS (the China Meteorological Assimilation Driving Datasets for the SWAT model) long time-series data (<http://www.cmads.org/>, accessed on 20 March 2022). The data were created using various data processing tools, such as LAPS\STMAS assimilation algorithm, resampling, and bilinear interpolation, which now contains CMADS V1.0, CMADS-L V1.0, CMADS-ST V1.0, and other datasets with different spatial resolution and time series length [31]. The CMADS meteorological data used in this study are derived from the CMADS-L V1.0 dataset, which contains 23 CMADS stations covering the Xinjiang River basin and its surroundings, with a spatial resolution of $1/3^\circ$ and a period of 1979 to 2018. Compared with traditional weather station data, CMADS weather data have the advantages of more uniform station distribution and easier data processing, and some studies have also shown that the CMADS-weather-data-driven SWAT model has a better simulation effect than the traditional SWAT model driven by weather station data [32,33].

3. Methodology

The research framework of this paper is shown in Figure 2. Firstly, the CMADS meteorological data were used to drive the SWAT model. Then, the blue and green water of the Xinjiang River basin can be separated based on the simulation results of the SWAT. Then, a statistical analysis of the multi-year average blue and green water and their spatial distribution characteristics in the basin was performed. The precipitation anomaly percentage was used to discriminate typical years, and the amount of blue and green water and their spatial distribution characteristics in different typical years were analyzed. The Mann–Kendall test and linear regression were employed to test the changing trend of the blue and green water. Finally, the influence of climatic factors and land use factors on the changing trends of the blue and green water were explored based on scenario simulation.

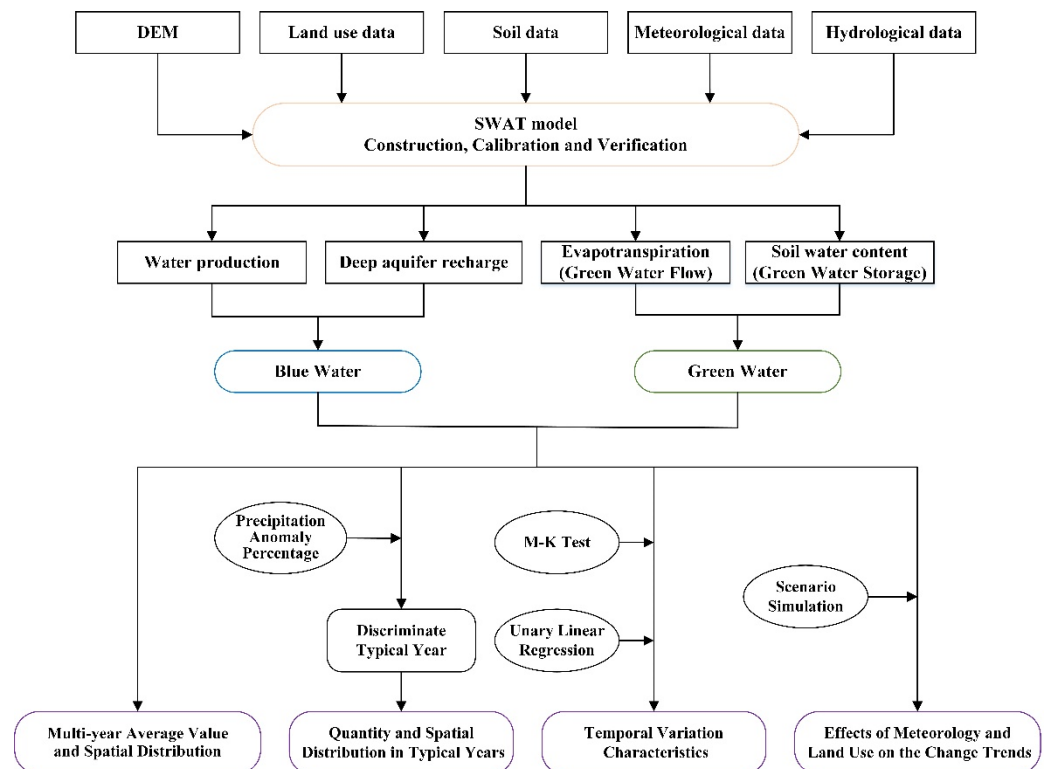


Figure 2. The research framework of spatiotemporal evaluation of blue and green water.

3.1. SWAT Model

The SWAT model is a distributed hydrological model with a strong physical mechanism. The model consists of several sub-modules and can be used for various simulations, such as runoff simulation, sediment change simulation, and non-point source pollution simulation [34,35]. The simulation of the hydrological cycle is mainly composed of land surface hydrological cycle calculation and river confluence calculation. The calculation of the land surface hydrological cycle includes the calculation of surface runoff, interflow, and deep groundwater recharge to the main river, and the calculation methods include the SCS (soilconservation service) curve method and the Green and Ampt method. The river confluence evolution of runoff from the river network to the basin outlet is calculated by methods such as the Muskingum method. The SWAT model can fully consider the heterogeneity in soil properties, land use, and topographic slope by dividing the whole basin into many hydrological response units (HRUs). The model uses HRU as the basic unit for simulation and aggregates the simulation results of HRU to sub-basins, and then aggregates the simulation results of each sub-basin to the total basin outlet [36,37]. The

simulation of land surface hydrological cycle processes by the SWAT model is based on the water balance equation of the soil layer as follows:

$$SW_t = SW_0 + \sum_{i=1}^t (R_{day} - Q_{surf} - E_a - W_{seep} - Q_{gw}) \quad (1)$$

where SW_t is the final water content of the soil, mm; SW_0 is the initial water content of the soil, mm; t is time, d; R_{day} is the precipitation of day i , mm; Q_{surf} is the surface runoff of day i , mm; E_a is the evaporation of day i , mm; W_{seep} is the infiltration and lateral flow at the bottom of soil profile of day i , mm; Q_{gw} is the subsurface water content of day i , mm. More information about the principles and structure of the SWAT model can be found in the literature [38,39].

3.2. Model Assessment

There are many calibration methods for watershed hydrological models, including generalized likelihood uncertainty estimation (GLUE), Sequential Uncertainty Fitting program (SUFI-2), Bayesian parameter estimation methods, and particle swarm optimization algorithms [17,40]. The latest more advanced calibration methods include deep learning (DL). Traditional calibration methods are stable and reliable but time-consuming (slow convergence of parameters). DL can narrow down the optimal range of model parameters in a short time, which greatly improves the efficiency of model calibration and also obtains good calibration results [40,41].

In this work, the model calibration and validation were performed in SWAT-CUP using the SUFI-2 [42]. The SUFI-2 can provide the optimal parameter values and optimal parameter intervals at 95% confidence intervals. Nash efficiency coefficient (NSE), correlation coefficient (R^2), percentage bias (PBIAS), and ratio of root mean square error to standard deviation (RSR) were used to evaluate the calibration effect and simulation effect of the SWAT model. NSE indicates the degree of similarity between the simulated and measured values of the model, and a larger value indicates a better simulation of the model. R^2 indicates the degree of consistency between the simulated value and the measured value in the changing trend: the closer its value is to 1, the closer the changing trend is to the same. PBIAS indicates the average relative size of the measured and simulated values, $PBIAS > 0$ means the measured value is large compared to the simulated value, and $PBIAS < 0$ means the measured value is small compared to the simulated value. RSR reflects the magnitude of the model calibration error, and a smaller value indicates a smaller calibration error. It is generally considered that the model simulation is good when $NSE > 0.75$, $R^2 > 0.8$, $|PBIAS| < 25\%$, and $RSR < 0.7$. The calculation equations of each indicator are as follows [43,44]:

$$NSE = 1 - \left[\frac{\sum_{i=1}^n (Q_1 - Q_2)^2}{\sum_{i=1}^n (Q_1 - \bar{Q}_1)^2} \right] \quad (2)$$

$$R^2 = \left\{ \frac{\left[\sum_{i=1}^n (Q_1 - \bar{Q}_1)(Q_2 - \bar{Q}_2) \right]}{\sqrt{\sum_{i=1}^n (Q_1 - \bar{Q}_1)^2 \sum_{i=1}^n (Q_2 - \bar{Q}_2)^2}} \right\}^2 \quad (3)$$

$$PBIAS = \left[100 \times \frac{\sum_{i=1}^n (Q_1 - Q_2)}{\sum_{i=1}^n Q_1} \right] \quad (4)$$

$$RSR = \sqrt{\frac{\sum_{i=1}^n (Q_1 - Q_2)^2}{\sum_{i=1}^n (Q_1 - \bar{Q}_1)^2}} \quad (5)$$

where Q_1 is the monthly measured runoff, m^3/s ; Q_2 is the monthly simulated runoff, m^3/s ; \bar{Q}_1 is the monthly measured average runoff, m^3/s ; \bar{Q}_2 is the monthly simulated average runoff, m^3/s ; n is the number of observations.

3.3. Blue Water, Green Water, and Green Water Coefficient

The SWAT model is able to separate the components of blue and green water at the HRU or sub-basin scale. Based on the output results of the SWAT model, blue water, green water, and green water coefficient can be directly calculated as follows:

$$BW = WYLD + DA_RCHG \quad (6)$$

$$GW = ET + SW \quad (7)$$

$$GWC = GW / (GW + BW) \quad (8)$$

where BW is blue water, mm; GW is green water, mm; GWC is the green water coefficient; $WYLD$ is the amount of water produced, mm; DA_RCHG is the amount of recharge of the deep aquifer, mm; ET is the actual evapotranspiration within the time step, which is also known as the green water flow, mm; SW is the soil water content, which is also known as the green water storage, mm.

3.4. Mann–Kendall Test

Mann–Kendall test is a non-parametric statistical test used for trend determination. The analysis results of this method are intuitive and reliable, and it has been widely used in hydrology, meteorology, and other fields. Supposing the time series $X = \{x_1, x_2, \dots, x_n\}$, the order column S_k can be calculated by:

$$S_k = \sum_{i=1}^k r_i \quad (k = 2, 3, \dots, n) \quad (9)$$

$$r_i = \begin{cases} 1 & (x_i > x_j) \\ 0 & (x_i \leq x_j) \end{cases}, \quad j = (1, 2, \dots, i) \quad (10)$$

where the order column S_k is the cumulative number of times that the value of the statistic r_i at the i th moment is greater than the value at the j th moment.

Then, the statistic UF_k can be calculated by:

$$UF_k = \frac{S_k - E(S_k)}{\sqrt{var(S_k)}} \quad (k = 2, 3, \dots, n) \quad (11)$$

$$E(S_k) = \frac{k(k-1)}{4} \quad (k = 2, 3, \dots, n) \quad (12)$$

$$var(S_k) = \frac{k(k-1)(2k+5)}{72} \quad (k = 2, 3, \dots, n) \quad (13)$$

where $UF_k = 0$; $E(S_k)$ is the mean value of S_k ; $var(S_k)$ is the variance of S_k .

Calculate the statistic UB_k :

$$\begin{cases} UB_k = -UF_k \\ k = n + 1 - k \end{cases} \quad (14)$$

Calculate Z :

$$\begin{cases} (S_k - 1) / \sqrt{var(S_k)} & S_k > 0 \\ 0 & S_k = 0 \\ (S_k + 1) / \sqrt{var(S_k)} & S_k < 0 \end{cases} \quad (15)$$

A positive value of Z indicates an increasing trend of the time series and vice versa. When $|Z| > 1.64$, it means that it has passed the 5% significance test [45]. At the same time, the trend of the series can also be judged by UB_k and UF_k . Set the significance level (e.g., $\alpha = 0.05$) and plot UB_k and UF_k curves; when the UB_k or UF_k curve is above the zero horizontal line, it indicates that the series has an increasing trend. On the contrary, when the UB_k or UF_k curve is below the zero horizontal line, it indicates that the series has a decreasing trend. If the two curves cross the critical line of significance ($U_{\alpha=0.05} = \pm 1.96$), it indicates a significant increasing or decreasing trend of the series [46].

3.5. Precipitation Anomaly Percentage

The precipitation anomaly percentage is a relatively simple method to determine the typical year of hydrology, and the method is more accurate for long time series with annual and monthly scales. The calculation formula is as follows:

$$P_a = \frac{P_i}{\bar{P}} \quad (i = 1, 2, \dots, n) \quad (16)$$

where P_a is the precipitation anomaly percentage; P_i is the precipitation of the i th year; \bar{P} is the average annual precipitation during the study period.

4. Results and Discussion

4.1. Runoff Simulation Based on SWAT Model

4.1.1. Model Evaluation

The simulation period for the SWAT model is from 1979 to 2016, among which the period 1979–1981 was used as the warm-up period and the periods 1982–2000 and 2001–2016 were the calibration and validation periods, respectively. In this study, 23 runoff-related parameters were calibrated, and three indicators, including NSE, R^2 , PBIAS, and RSR, were used to evaluate the simulation effect of the SWAT. The values of each indicator during model calibration and validation periods are shown in Figure 3. It can be seen that the SWAT model exhibits a rather good performance; hence, the blue and green water in the Xinjiang River basin will be separated based on the simulation results of the model.

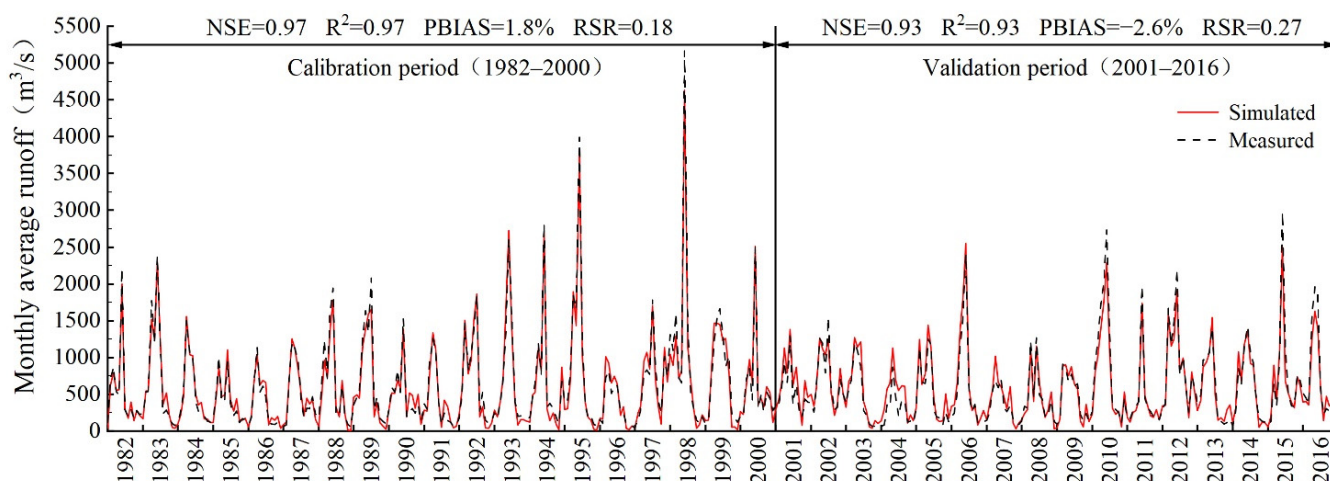


Figure 3. Evaluation of the simulation effect of the SWAT model in the calibration and validation periods.

SWAT-CUP can also apply T-stat and p -value to analyze the sensitivity of each parameter. The value of T-stat represents the degree of sensitivity of the parameter, and a larger absolute value means that the parameter is more sensitive. The p -value represents the significance of the parameter sensitivity, and a value closer to zero means that the parameter sensitivity is more significant. The twelve most sensitive parameters in this study are listed in Table 1.

4.1.2. Multi-Year Average Blue and Green Water and Their Spatial Distribution Characteristics

The annual average precipitation, blue water, green water, green water flow, green water storage, and green water coefficient of the Xinjiang River basin from 1982 to 2016 were 1867 mm, 1138 mm, 829 mm, 729 mm, 100 mm, and 0.42, respectively. The annual average blue water is about 1.38 times green water; hence, the water resources in the basin are dominated by blue water. As can be seen from Figure 4, the interannual variability in blue water is roughly consistent with that of precipitation. Green water is dominated by green water flow, which accounts for about 88% of the total green water, and green water

storage accounts for about 12%. The interannual variation in green water, green water flow, and green water storage is relatively small, and green water and green water flow present similar variations. The interannual variation in the green water coefficient is large, with the smallest coefficient of 0.28 in 1998 when the blue water was about 2.61 times the green water and the largest coefficient of 0.57 in 2011 when the blue water was about 0.75 times the green water.

Table 1. Partial sensitive parameters and their values after model calibration.

Parameter Name	Parameter Meaning	T-Stat	p-Value	Final Value	Parameter Range
ALPHA_BNK	Base-flow factor	16.441	0.000	0.338	0.234–0.374
SFTMP	Snow melting temperature	−3.674	0.000	−0.580	−0.727–4.083
CN2	Number of SCS runoff curves under humid conditions	1.727	0.084	0.546	0.464–0.642
SMFMX	Maximum snow melt rate	1.704	0.089	9.407	8.757–10.000
ALPHA_BF	Base-flow coefficient	−1.686	0.092	0.617	0.484–0.628
CH_K2	Hydraulic conductivity of the main river channel	−1.664	0.096	49.476	41.883–50.000
REVAPMN	Shallow groundwater depth for guaranteed evaporation	1.491	0.136	303.279	272.57–398.68
SMTMP	Snow melt accumulation temperature	−1.166	0.244	−0.580	−0.727–4.083
SMTMN	Minimum snow melt factor	0.951	0.342	2.391	1.734–3.773
CH_N2	Manning factor of the main river channel	0.933	0.351	0.278	0.266–0.300
OV_N	Manning factor for overland flow	−0.855	0.392	0.127	−0.156–0.171
GW_REVAP	Groundwater re-evaporation coefficient	−0.739	0.460	0.693	0.546–0.720

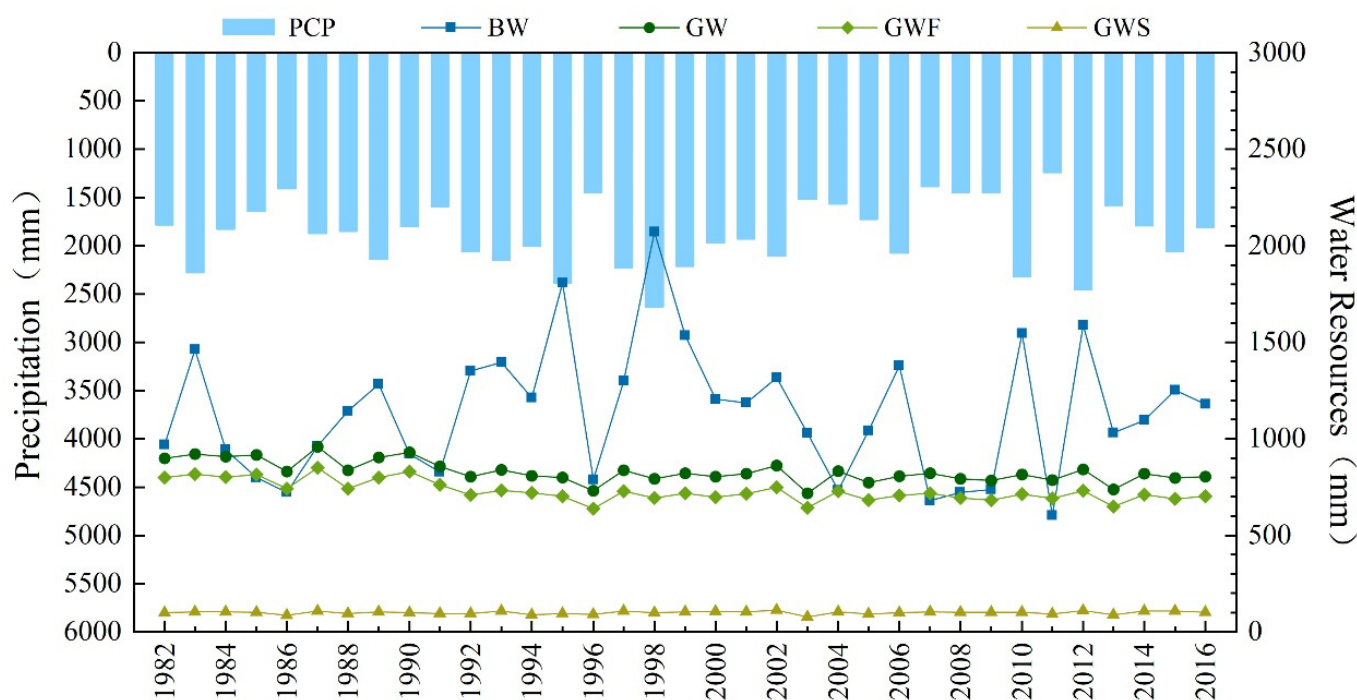


Figure 4. Interannual variation in precipitation (PCP), blue water (BW), green water (GW), green water flow (GWF), and green water storage (GWS) in the Xinjiang River basin.

The spatial distribution characteristics of multi-year average precipitation, blue water, and green water in the Xinjiang River basin are shown in Figure 5. It can be seen that the spatial distribution characteristics of blue water are similar to precipitation, and the blue water in the south-central part of the basin is obviously more than in other parts. The spatial distribution characteristics of green water and green water flow are similar, and the central basin covers both the most green water and green water flow, followed by the

northeast hills, southeast hills, northwest plains, and southwest hills. Green water storage is relatively evenly distributed throughout the basin, with most areas in the basin having green water storage between 95 and 104 mm, and very few areas being below 85 mm. The spatial distribution characteristics of the green water coefficient are opposite to that of blue water; the green water coefficient is smaller in areas with abundant blue water and larger in areas with little blue water. Green water is particularly important for maintaining the ecological balance in areas with large green water coefficients [10].

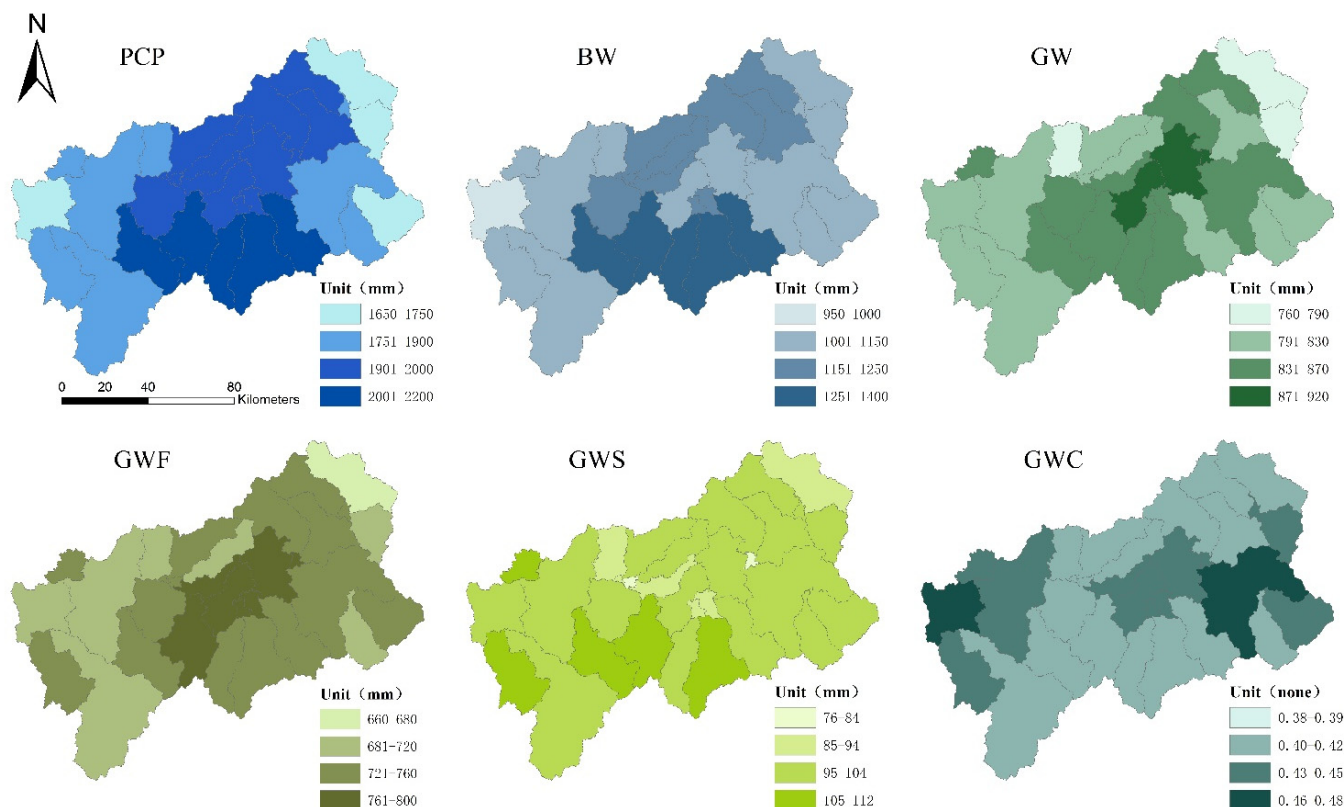


Figure 5. Spatial distribution characteristics of annual average precipitation (PCP), blue water (BW), green water (GW), green water flow (GWF), green water storage (GWS), and green water coefficient (GWC) in the Xinjiang River basin.

4.2. Blue and Green Water in Typical Years

4.2.1. The Amount of Blue and Green Water in Typical Years

In this study, the precipitation anomaly percentage (P_a) was used to discriminate the typical years, and the years within the study period were classified into five typical years based on P_a values, including wet year ($P_a > 20\%$), sub-humid year ($10\% < P_a \leq 20\%$), normal year ($-10\% \leq P_a \leq 10\%$), sub-arid year ($-20\% \leq P_a < -10\%$), and dry year ($P_a < -20\%$). As can be seen from Figure 6, wet years, sub-humid years, and sub-arid years each include 5 years, normal years include 14 years, and dry years include 6 years. The sum of the proportion of wet years and dry years is nearly 1/3, and the proportion of extreme precipitation years is high. At the same time, it can be found that there are frequent rapid transitions between dry and wet between 1995 and 1998 and between 2009 and 2013.

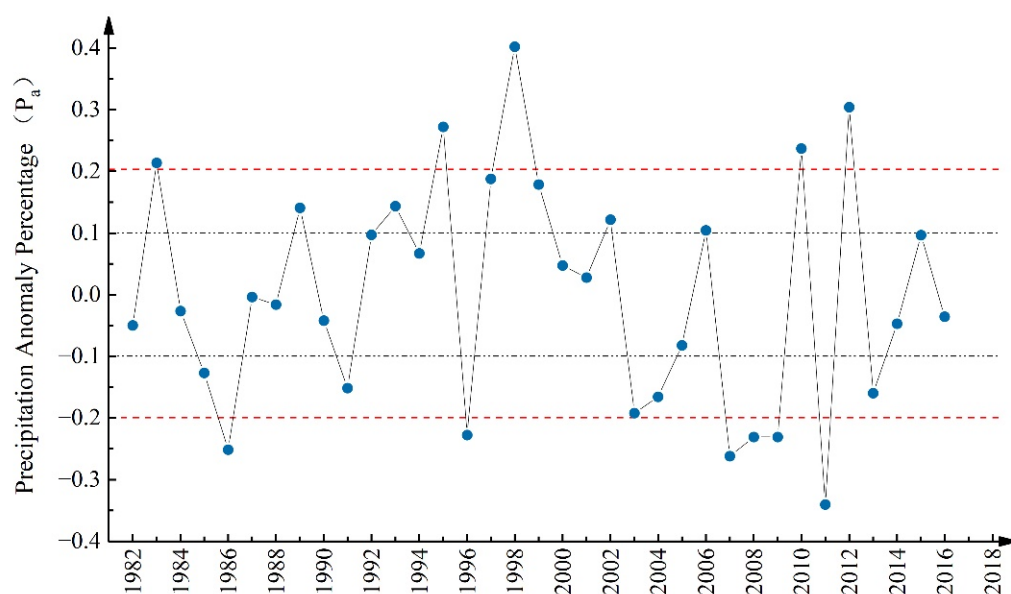


Figure 6. Discriminant results of typical years using the precipitation anomaly percentage.

In order to avoid the one-sidedness and errors brought by the selection of a single typical year to the analysis results, we improved the previous research method by counting the multi-year average data for each type of typical year. The multi-year average blue and green water for typical years in the Xinjiang River basin are shown in Figure 7. The amount of blue water in the wet years is 2412 mm, which is about 1.5 times that in normal years and 2.4 times that in dry years. This analysis result is similar to the Ganjiang River basin, which is also a sub-basin of the Poyang Lake basin (the blue water in Ganjiang River basin is about 1.54 times normal years and 2.01 times dry years [19]). The variation in green water in different typical years is smaller compared with blue water, and the green water in sub-humid years is about 1.08 times that in dry years. Green water flow occupies the vast majority of green water (green water flow accounts for about 88% of green water), with an average of about 720 ± 30 mm per year. The green water coefficient is 0.33 in wet years, 0.43 in normal years, and 0.53 in dry years. The green water coefficients of the Xinjiang River basin were 0.33, 0.43, and 0.53 in wet, normal, and dry years, respectively, which were significantly lower than those of the Ganjiang River basin (0.40 in wet years, 0.51 in normal years, and 0.57 in dry years). This is related to the more abundant precipitation in the Xinjiang basin because it is closer to the ocean. It can be seen that the proportion of green water in dry years is significantly larger than that in wet years; hence, green water is particularly important for maintaining ecosystem balance in dry years.

4.2.2. Spatial Distribution Characteristics of Blue and Green Water in Typical Years

Three types of typical years were selected to analyze the spatial distribution characteristics of blue and green water in the Xinjiang River basin. It can be seen from Figure 8 that the spatial distribution characteristics of blue water in wet years, normal years, and dry years are similar to those of precipitation. The central basin has the most abundant blue water, and the southeast mountains and northwest plains have the least blue water. In wet years, the blue water in the basin presents an uneven distribution such that the central basin has the most blue water of about 1772 mm while the northwest plain has the least blue water of only 1558 mm. In normal years, the central basin has the most blue water of about 1221 mm, and the northwest plain has the least blue water of about 994 mm. In dry years, the blue water of the basin is more evenly distributed than in wet and normal years.

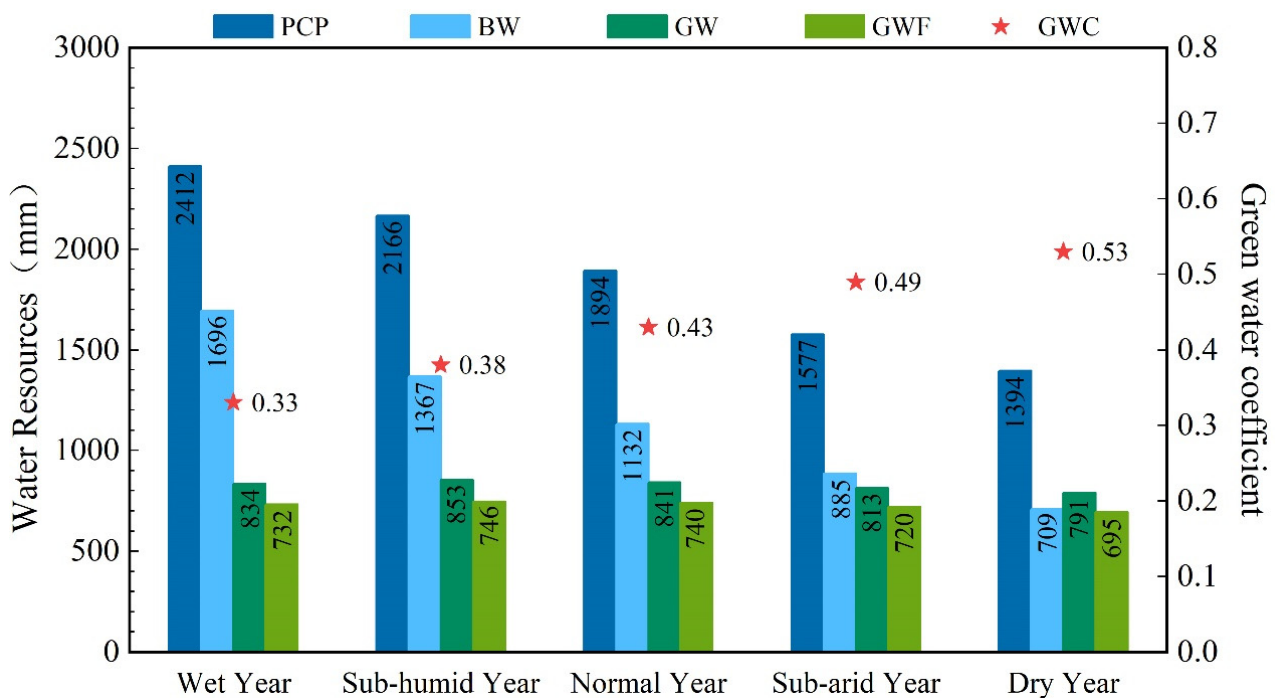


Figure 7. The amount of precipitation (PCP), blue water (BW), green water (GW), green water flow (GWF), and green water coefficient (GWC) for typical years.

The spatial distribution characteristics of green water are similar in the three types of typical years. In wet years, the central basin has the most green water of about 840 mm, and the southwest hills have the least green water of about 821 mm. In normal years, the green water in most parts of the basin is more than 800 mm, and the uneven spatial distribution of green water in the whole basin is the most obvious in three types of typical years. In dry years, the green water is significantly reduced, and the green water in the whole basin is less than 820 mm.

The spatial distribution characteristics of the green water coefficient are exactly opposite to those of the blue water. It is shown that the green water coefficients in the southeast and northwest are obviously larger than that in the central basin. In wet years, the green water coefficient is between 0.32 and 0.35 in all parts of the basin, and there is little difference in green water coefficient across the basin. In normal years, the green water coefficient is in the range of 0.41 to 0.46 throughout the basin, with small differences from place to place. In dry years, the green water coefficient in the whole basin varies from 0.51 to 0.58, and green water is the dominant water resource in the whole basin. The decrease in precipitation and the increase in evapotranspiration lead to a significant increase in the green water coefficient in dry years.

The Xinjiang River basin has abundant topographic features, consisting of forest land, basin, and plain. Its spatial distribution of precipitation is affected jointly by geographical location, topography, and climatic conditions. The spatial distribution characteristic of blue water is dominated by precipitation, while that of green water is associated with soil types and land cover in addition to precipitation. The blue water in the middle of the basin has always been prominent in typical years for the precipitation in most of the middle reach. The green water in the middle reach is possibly related to the regional evapotranspiration increased by flat terrain, extensive plowland, and grassland in the middle reach apart from the distribution characteristic of precipitation.

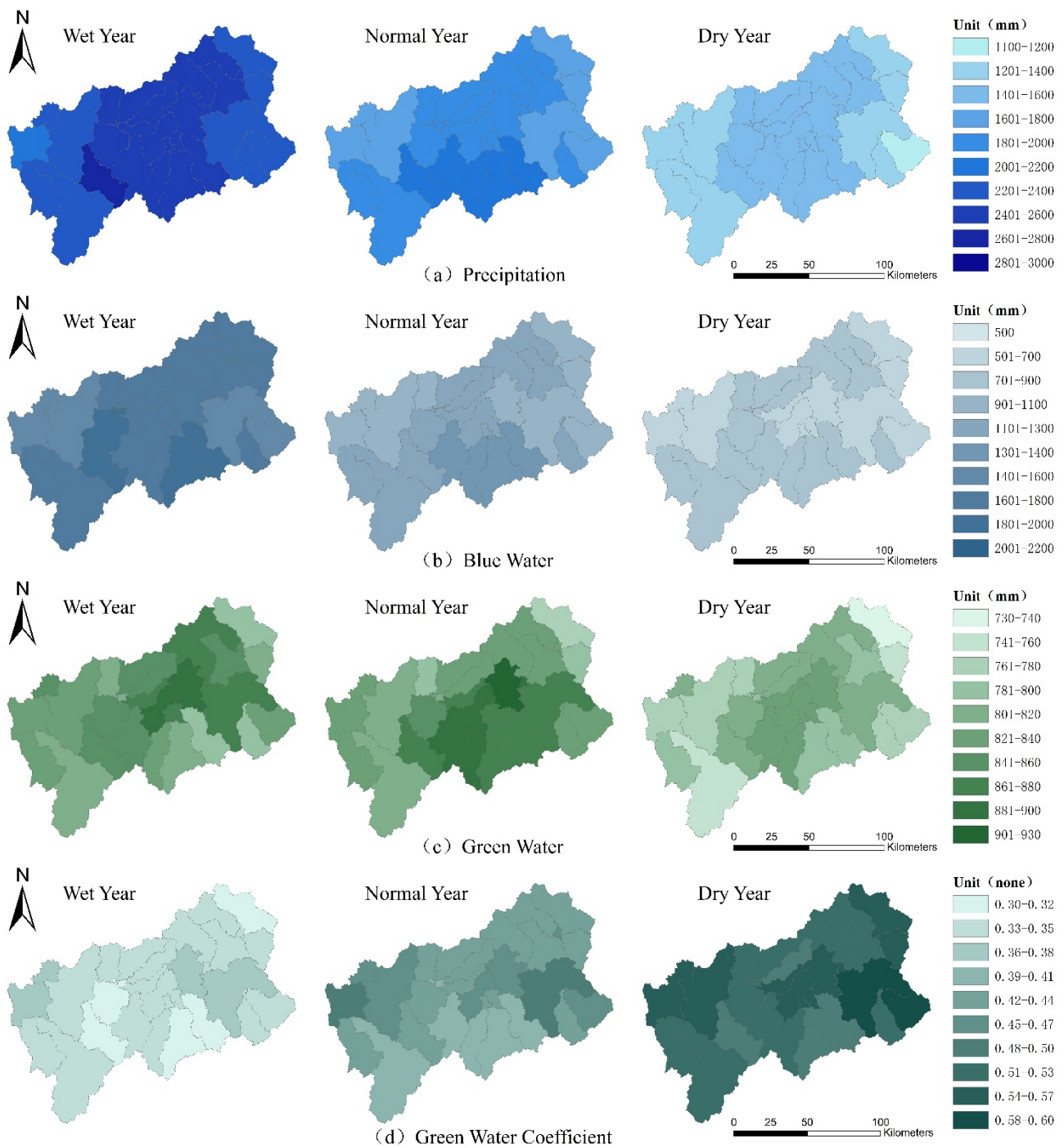


Figure 8. Spatial distribution characteristics of precipitation (PCP), blue water (BW), green water (GW), and green water coefficient (GWC) in typical years.

4.3. Temporal Variation Characteristics of Blue and Green Water

Meteorological factors and land cover are two important factors that may affect the temporal change characteristics of blue and green water. Before studying the temporal change characteristics of blue and green water, it is necessary to analyze the changes in meteorological factors and land use in the whole basin.

4.3.1. Changes in Precipitation and Temperature

This study applied the Mann–Kendall (MK) test and linear regression to detect the changes in the precipitation and temperature of the basin. It can be seen from Figure 9 that

the Z value of the MK test for precipitation is -0.072 , which fails to pass the 5% significance test and shows a slight decrease. The Z value of the MK test for average temperature is 0.405 , which passed the 5% significance test and shows a relatively significant increase. The analysis result of linear regression shows that precipitation decreased at a rate of 3.51 mm/year, and average temperature increased at a rate of 0.026 °C/year.

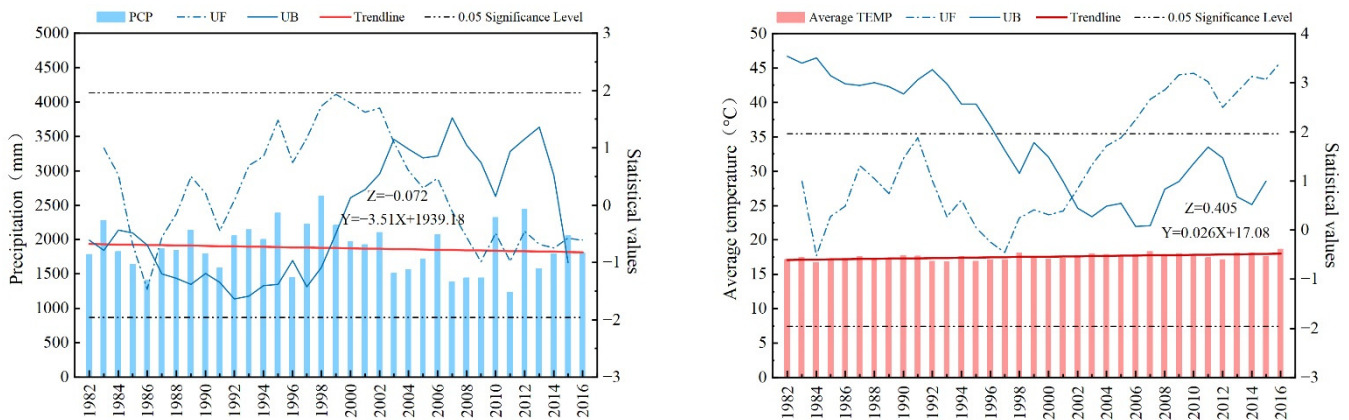


Figure 9. MK test results of precipitation (PCP) and the average temperature (TEMP) in the Xinjiang River basin.

4.3.2. Land Use Change

The land use of the Xinjiang River basin in 1990 and 2010 is shown in Table 2. It can be seen that the land use of the Xinjiang River basin is dominated by woodland and plowland, accounting for about 67% and 26% of the total area of the basin, respectively. The grassland, water area, construction land, and bare land are all relatively small, which are all no more than 4% of the total area of the basin. The area of construction land in the whole basin increased rapidly between 1990 and 2010, with an increase of more than 75 km² and an area change rate of 0.5%. From 1990 to 2010, the area of plowland reduced by more than 65 km² and the area of grassland reduced by more than 25 km², part of which were transformed into construction land, woodland, and water area. The proportion of bare land area in the basin is negligible and has not demonstrated a significant change.

Table 2. Land use changes in the Xinjiang River basin from 1990 to 2010.

Land Use Type		Plowland	Woodland	Grassland	Water Area	Construction Land	Bare Land
1990	Area (km ²)	3969.0	10,308.0	599.0	237.0	180.0	3.0
	Area proportion (%)	25.95	67.39	3.92	1.55	1.18	0.02
2010	Area (km ²)	3903.0	10,319.0	573.0	242.0	257.0	2.0
	Area proportion (%)	25.52	67.46	3.75	1.58	1.68	0.01
Change amount (km ²)		-66.0	11.0	-26.0	5.0	77.0	-1.0
Percentage of change area (%)		-0.43	0.07	-0.17	0.03	0.50	-0.01

4.3.3. Temporal Variation Characteristics of Blue and Green Water

The MK test was used to analyze the trend of blue water, green water, green water flow, and green water coefficient in the Xinjiang River basin, and the results are shown in Figure 10. The Z value of the MK test for blue water is -0.008 , which fails to pass the 5% significance test and shows a very slight decrease. The Z values of the MK test for green water and green water flow are both less than -1.64 , which suggests significant decreasing trends at a 5% significance level. Meanwhile, it can be seen from the UF curve that the UF values of green water and green water flow are all less than zero most of the time and are positive only in some years from 1983 to 1990, which indicates that green water and

green water flow had a decreasing trend most of the time. The UF and UB curves of green water and green water flow have an intersection point in 1992, and the intersection point is within the confidence interval, so it indicates that green water and green water flow have been decreasing since 1992. The Z value of the MK test for the green water coefficient is -0.096 , which indicates a slight decrease and failed to pass the 5% significance test. It can also be found that the results of linear trends of blue water, green water, and green water coefficients are consistent with the results of the MK test.

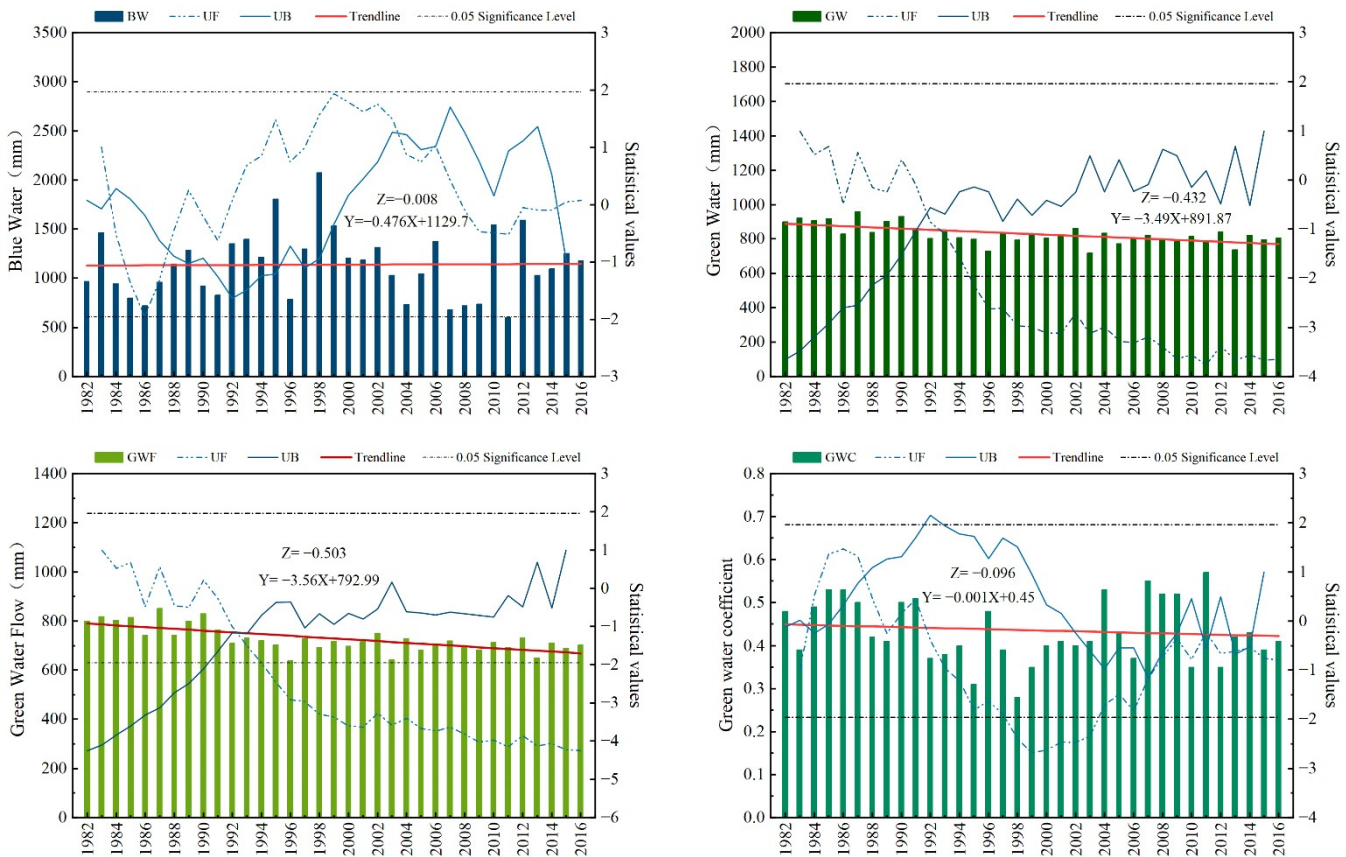


Figure 10. MK test results of blue water (BW), green water (GW), green water flow (GWF), and green water coefficient (GWC).

4.4. Analysis of the Reasons for the Changing Trend of Blue and Green Water

In order to further explore the factors that induce the trend of blue and green water in the Xinjiang River basin, this study sets three different scenarios of land use and climate conditions (scenario settings are shown in Table 3). By comparing the simulation results of scenario 1 and scenario 2, which have the same climatic conditions but different land use, we can explore the influence of land use on the changing trend of blue and green water. By comparing the simulation results of scenario 2 and scenario 3, which have the same land use but different climatic conditions, we can explore the influence of climatic factors on the changing trend of blue and green water. The simulation results are shown in Figure 11. It can be found that the simulation results of scenario 1 and scenario 2 are relatively close, but the simulation results of scenario 2 and scenario 3 are quite different. Therefore, we can conclude that climatic factors have a greater impact on blue and green water than land use and are the dominant reason for the temporal variation characteristics of blue and green water.

Table 3. Meteorological change and land use change scenario setting.

Scenario Setting	Land Use Data	Meteorological Data
Scenario 1	1990	1979–2000
Scenario 2	2010	1979–2000
Scenario 3	2010	2001–2016

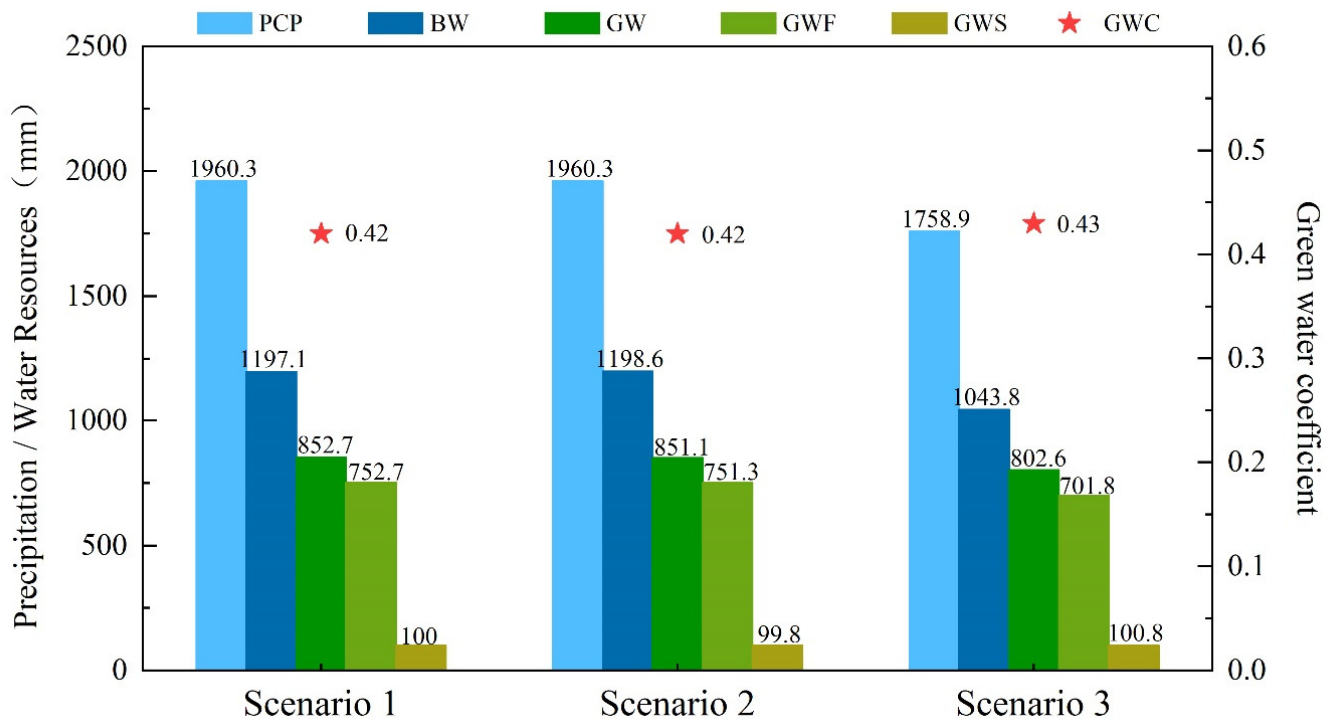


Figure 11. Precipitation (PCP), blue water (BW), green water (GW), green water flow (GWF), green water storage (GWS), and green water coefficient (GWC) under different scenarios.

At the same time, it can be seen from Figure 11 that blue water in scenario 2 is 1.5 mm more than that in scenario 1, which may be related to the change in land use. The increase in construction land leads to the increase in impervious surface area, and the rain falling on the impervious surface cannot penetrate the soil and directly forms surface runoff, which leads to a slight increase in the blue water. It can also be found that the green water in scenario 2 is 1.6 mm less than that in scenario 1, which may be related to the decrease in the area of evapotranspiration in the basin. From 1990 to 2010, the increase in construction land and the decrease in plowland and grassland in the basin led to partial precipitation that could not be converted into ecosystem water through infiltration and vegetation interception, which led to a slight decrease in the green water. At the same time, the small difference between the simulation results of scenario 1 and scenario 2 is related to the small change in land use in the Xinjiang River basin. Compared to the simulation results of scenario 2 and scenario 3, it can be found that the blue water and green water in scenario 3 are 154.8 mm and 48.5 mm less than those in scenario 2, respectively, which is related to the decrease in precipitation in scenario 3. The decrease in precipitation directly leads to the decrease in surface runoff and evapotranspiration, which leads to a significant decrease in both blue and green water.

According to the above analysis, it is apparent that the decrease in blue water in the basin is related to the decrease in precipitation, while the decrease in green water is related to the decrease in precipitation and evapotranspiration area, and the decrease in precipitation is the main reason for the decrease in green water.

5. Conclusions

In this study, we applied CMADS long time series (1979–2018) meteorological data to the study of blue and green water and conducted a comprehensive analysis of the spatiotemporal distribution characteristics of blue and green water in the Xinjiang River basin based on the simulation results of the SWAT model. Firstly, the annual average blue and green water and their spatial distribution characteristics in the basin were quantitatively evaluated. Then, the precipitation anomaly percentage was used to discriminate the typical years, and the blue and green water in typical years were assessed. The variation trend of blue and green water was analyzed by using the MK test and linear regression. Finally, three different scenarios were set up to explore the effects of climatic factors and land use on the trend of the blue and green water. The following conclusions are drawn from this study:

(1) The SWAT model driven by CMADS long-term meteorological data has achieved satisfactory simulation results, with an NSE of 0.97 in the calibration period and an NSE of 0.93 in the validation period.

(2) The annual average blue water, green water, green water flow, green water storage, and green water coefficient of the basin were 1138 mm, 829 mm, 729 mm, 100 mm, and 0.42, respectively. The water resources in the basin are dominated by the blue water. However, the annual average green water coefficient in dry years is 0.53, and green water is the main water resource in dry years. Green water flow accounts for about 88% of the total green water and is the main part of the green water.

(3) The spatial distribution of blue and green water in the basin is uneven, with the central basin having significantly more blue and green water than other parts of the basin. The spatial distribution of the blue water is consistent with that of precipitation, but the spatial distribution of the green water coefficient is the opposite to that of precipitation. Compared with wet years and normal years, the distribution of the blue and green water in the basin is more uniform in dry years.

(4) The blue water in the Xinjiang River basin shows a slight decreasing trend, and the green water shows a significant decreasing trend. The decrease in blue water is mainly related to the decrease in precipitation. The decrease in evaporable water and evapotranspiration area resulted in a decrease in the green water. The results of the scenario simulation found that climatic factors have a greater influence on the change trends in the blue and green water compared to land use and are the dominant cause of the temporal variation characteristics of blue and green water.

Author Contributions: Conceptualization, X.Z.; methodology, X.Z.; software, X.Z.; validation, X.Z.; formal analysis, X.Z. and C.J.; investigation, X.Z.; resources, X.Z., C.J., J.H., Z.N., J.S. and Z.L.; data curation, X.Z.; writing—original draft preparation, X.Z.; writing—review and editing, X.Z. and C.J.; visualization, X.Z.; supervision, C.J.; project administration, X.Z. and C.J.; funding acquisition, C.J. and T.W. All authors have read and agreed to the published version of the manuscript.

Funding: This research is financially supported jointly by the Open Research Fund of Jiangxi Provincial Key Laboratory of Water Resources and Environment of Poyang Lake, Jiangxi Provincial Institute of Water Sciences (2020GPSYS06), and the National Natural Science Foundation of China (NSFC Grants 51809243, 41890822, and 52109024).

Conflicts of Interest: The authors declare no conflict of interest.

References

1. Li, W.T.; Yang, X.L.; Ren, L.L.; Gao, T.; Gu, Y.J. Spatial and temporal distribution characteristics of blue and green water resources in the Yellow River source region based on SWAT model. *China Rural. Water Hydropower* **2021**, *8*, 59–66. (In Chinese)
2. Gohar, A.A.; Cashman, A. A methodology to assess the impact of climate variability and change on water resources, food security and economic welfare. *Agric. Syst.* **2016**, *147*, 51–64. [[CrossRef](#)]
3. Lyu, L.T.; Wang, X.R.; Jiang, Y.; Sun, C. Research on spatial and temporal distribution features of green and blue water in Dongjiang River Basin based on SWAT model. *Water Resour. Prot.* **2017**, *33*, 53–60. (In Chinese)

4. Wu, J.; Deng, G.N.; Zhou, D.M.; Zhu, X.Y.; Ma, J.; Cen, G.Z.; Jin, Y.L.; Zhang, J. Effects of climate change and land-use changes on spatiotemporal distributions of blue water and green water in Ningxia, Northwest China. *J. Arid Land*. **2021**, *13*, 674–687. [[CrossRef](#)]
5. Falkenmark, M. Land-water linkages: A synopsis. *FAO Land Water Bull.* **1995**, *1*, 15–16.
6. Xu, Z.X.; Zuo, D.P. Scientific assessment of water resources with broaden thoughts: A case study on the blue and green water resources in the Wei River Basin. *South-North Water Transf. Water Sci. Technol.* **2013**, *11*, 12–16. (In Chinese)
7. Liu, J.; Yang, H.; Gosling, S.N.; Kumm, M.; Flörke, M.; Pfister, S.; Hanasaki, N.; Wada, Y.; Zhang, X.; Zheng, C.; et al. Water scarcity assessments in the past, present, and future. *Earth's Future* **2017**, *5*, 545–559. [[CrossRef](#)]
8. Falkenmark, M.; Rockström, J. The New Blue and Green Water Paradigm: Breaking New Ground for Water Resources Planning and Management. *J. Water Resour. Plan. Manag.* **2006**, *132*, 129–132. [[CrossRef](#)]
9. Zhao, A.Z.; Zhao, Y.L.; Liu, X.F.; Zhu, X.; Pan, Y.; Chen, S. Impact of human activities and climate variability on green and blue water resources in the Weihe River Basin of Northwest China. *Sci. Geogr. Sin.* **2016**, *36*, 571–579. (In Chinese)
10. Zang, C.F.; Liu, J.G.; van der Velde, M.; Kraxner, F. Assessment of spatial and temporal patterns of green and blue water flow under natural conditions in inland river basins in Northwest China. *Hydrol. Earth Syst. Sci.* **2012**, *16*, 2859–2870. [[CrossRef](#)]
11. Lan, Y.; Zhao, G.; Zhang, Y.; Wen, J.; Hu, X.; Liu, J.; Gu, M.; Chang, J.; Ma, J. Response of runoff in the headwater region of the Yellow River to climate change and its sensitivity analysis. *J. Geogr. Sci.* **2010**, *20*, 848–860. [[CrossRef](#)]
12. Veettil, A.V.; Mishra, A.K. Water security assessment using blue and green water footprint concepts. *J. Hydrol.* **2016**, *542*, 589–602. [[CrossRef](#)]
13. Padowski, J.C.; Jawitz, J.W. Water availability and vulnerability of 225 large cities in the United States. *Water Resour. Res.* **2012**, *48*, W12529. [[CrossRef](#)]
14. Rodrigues, D.B.B.; Gupta, H.V.; Mendiondo, E.M. A Blue/Green Water-based Accounting Framework for Assessment of Water Security. *Water Resour. Res.* **2014**, *50*, 7187–7205. [[CrossRef](#)]
15. Zang, C.F.; Liu, J.G.; Gerten, D.; Jiang, L. Influence of human activities and climate variability on green and blue water provision in the Heihe River Basin, NW China. *J. Water Clim. Change* **2015**, *6*, 800–815. [[CrossRef](#)]
16. Yuan, Z.; Xu, J.; Meng, X.; Wang, Y.; Yan, B.; Hong, X. Impact of Climate Variability on Blue and Green Water Flows in the Erhai Lake Basin of Southwest China. *Water* **2019**, *11*, 424. [[CrossRef](#)]
17. Zhao, A.; Zhu, X.; Liu, X.; Pan, Y.; Zuo, D. Impacts of land use change and climate variability on green and blue water resources in the Weihe River Basin of northwest China. *Catena* **2016**, *137*, 318–327. [[CrossRef](#)]
18. Yang, X.L.; Li, W.T.; Ren, L.L.; Gao, T.; Ma, H. Simulation of the response of blue and green water to land use change in the Weihe River Basin. *Trans. Chin. Soc. Agric. Eng. (Trans. CSAE)* **2021**, *37*, 268–276. (In Chinese)
19. Li, W.T.; Yang, X.L.; Ren, L.L. Land use and climate change effects on blue/green water in the Ganjiang River Basin. *Water Resour. Prot.* **2021**, 1–14. (In Chinese)
20. Liu, Q.; Mcvillar, T.R. Assessing climate change induced modification of panman potential evaporation and runoff sensitivity in a large water-limited basin. *J. Hydrol.* **2012**, *464*, 352–362. [[CrossRef](#)]
21. Zuo, D.; Xu, Z.; Peng, D.; Song, J.; Cheng, L.; Wei, S.; Abbaspour, K.C.; Yang, H. Simulating spatiotemporal variability of blue and green water resources availability with uncertainty analysis. *Hydrol. Processes* **2014**, *29*, 1942–1955. [[CrossRef](#)]
22. Yuan, Z.; Xu, J.; Wang, Y. Historical and future changes of blue water and green water resources in the Yangtze River source region, China. *Theor. Appl. Climatol.* **2019**, *138*, 1035–1047. [[CrossRef](#)]
23. Guo, L.P.; Mu, X.M.; Hu, J.M.; Gao, P.; Zhang, Y.-F.; Liao, K.-T.; Bai, H.; Chen, X.-L.; Song, Y.-J.; Jin, N.; et al. Assessing Impacts of Climate Change and Human Activities on Streamflow and Sediment Discharge in the Ganjiang River Basin (1964–2013). *Water* **2019**, *11*, 1679. [[CrossRef](#)]
24. Hu, Y.; Peng, J.; Liu, Y.; Tian, L. Integrating ecosystem services trade-offs with paddy land-to-dry land decisions: A scenario approach in Erhai Lake basin, southwest China. *Sci. Total Environ.* **2018**, *625*, 849–860. [[CrossRef](#)]
25. Zhu, K.; Xie, Z.; Zhao, Y.; Lu, F.; Song, X.; Li, L.; Song, X. The Assessment of Green Water Based on the SWAT Model: A Case Study in the Hai River Basin, China. *Water* **2018**, *10*, 798. [[CrossRef](#)]
26. Ye, X.C.; Wu, J.; Li, X.H. Compound driving mechanism of water level change in the Poyang Lake. *Sci. Geogr. Sin.* **2022**, *42*, 352–361. (In Chinese)
27. Qi, L.Y.; Huang, J.C.; Qi, H.; Gao, J.; Wang, S.; Guo, Y. Assessing Aquatic Ecological Health for Lake Poyang, China: Part II Index Application. *Water* **2018**, *10*, 909. [[CrossRef](#)]
28. Zhang, Z.X.; Huang, Y.H.; Xu, C.Y.; Chen, X.; Moss, E.M.; Jin, Q.; Bailey, A.M. Analysis of Poyang Lake water balance and its indication of river-lake interaction. *SpringerPlus* **2016**, *5*, 1555. [[CrossRef](#)]
29. Li, Y.L.; Zhang, Q.; Werner, A.D.; Yao, J. Investigating a complex lake-catchment-river system using artificial neural networks: Poyang Lake (China). *Hydrol. Res.* **2015**, *46*, 912–928. [[CrossRef](#)]
30. Zhang, Y.Q.; Chen, C.C.; Yang, X.H.; Ding, X.W.; Zhang, J. Studies of runoff response to land use change in Xinjiang basin. *Water Resour. Power* **2013**, *8*, 27–30. (In Chinese)
31. Meng, X.; Wang, H.; Chen, J. Profound Impacts of the China Meteorological Assimilation Driving Datasets for the SWAT Model (CMADS). *Water* **2019**, *11*, 832. [[CrossRef](#)]
32. Meng, X.; Wang, H.; Lei, X.; Cai, S.; Wu, H.; Ji, X. Hydrological modeling in the Manas River Basin using soil and water assessment tool driven by CMADS. *Teh. Vjesn. Tech. Gaz.* **2017**, *24*, 525–534.

33. Meng, X.; Wang, H. Significance of the China Meteorological Assimilation Driving Datasets for the SWAT Model (CMADS) of East Asia. *Water* **2017**, *9*, 765. [[CrossRef](#)]
34. Jayakrishnan, R.; Srinivasan, R.; Santhi, C.; Arnold, J.G. Advances in the application of the SWAT model for water resources management. *Hydrol. Processes* **2005**, *19*, 749–762. [[CrossRef](#)]
35. Faramarzi, M.; Abbaspour, K.C.; Vaghefi, S.A.; Farzaneh, M.R.; Zehnder, A.J.; Srinivasan, R.; Yang, H. Modeling impacts of climate change on freshwater availability in Africa. *J. Hydrol.* **2013**, *480*, 85–101. [[CrossRef](#)]
36. Wang, Y.P.; Jiang, R.G.; Xie, J.C. Soil and Water Assessment Tool (SWAT) Model: A Systemic Review. *J. Coast. Res.* **2019**, *93*, 22–30. [[CrossRef](#)]
37. Guzha, A.C.; Rufino, M.C.; Okoth, S.; Jacobs, S.; Nóbrega, R. Impacts of land use and land cover change on surface runoff, discharge and low flows: Evidence from East Africa. *J. Hydrol. Reg. Stud.* **2018**, *15*, 49–67. [[CrossRef](#)]
38. Arnold, J.G.; Moriasi, D.N.; Gassman, P.W.; Abbaspour, K.C.; White, M.J.; Srinivasan, R.; Santhi, C.; Harmel, R.D.; van Griensven, A.; Kannan, K.; et al. SWAT: Model use, calibration, and validation. *Trans. ASABE* **2012**, *55*, 1491–1508. [[CrossRef](#)]
39. Akoko, G.; Le, T.H.; Gomi, T.; Kato, T. A Review of SWAT Model Application in Africa. *Water* **2021**, *13*, 1313. [[CrossRef](#)]
40. Mudunuru, M.K.; Son, K.; Jiang, P.; Chen, X. SWAT Watershed Model Calibration using Deep Learning. *arXiv* **2021**, arXiv:2110.03097.
41. Breen, K.H.; James, S.C.; White, J.D.; Allen, P.M.; Arnold, J.G. A hybrid artificial neural network to estimate soil moisture using swat+ and SMAP data. *Mach. Learn. Knowl. Extr.* **2020**, *2*, 283–306. [[CrossRef](#)]
42. Ozdemir, A.; Leloglu, U.M. A fast and automated hydrologic calibration tool for SWAT. *Water Environ. J.* **2018**, *33*, 488–498. [[CrossRef](#)]
43. Almeida, R.A.; Pereira, S.B.; Pinto, D.B.F. Calibration and Validation of The SWAT Hydrological Model for The Mucuri River Basin. *Eng. Agrícola* **2018**, *38*, 55–63. [[CrossRef](#)]
44. Zhang, X.; Srinivasan, R.; Van Liew, M. Multi-Site Calibration of the SWAT Model for Hydrologic Modeling. *Trans. ASABE* **2008**, *51*, 2039–2049. [[CrossRef](#)]
45. Yue, S.; Wang, C. The Mann-Kendall Test Modified by Effective Sample Size to Detect Trend in Serially Correlated Hydrological Series. *Water Resour. Manag.* **2004**, *18*, 201–218. [[CrossRef](#)]
46. Gocic, M.; Trajkovic, S. Analysis of changes in meteorological variables using Mann-Kendall and Sen's slope estimator statistical tests in Serbia. *Glob. Planet. Chang.* **2013**, *100*, 172–182. [[CrossRef](#)]